Advances in Applied Mathematics and Mechanics
Adv. Appl. Math. Mech., Vol. **18**, No. 1, pp. 222-241

DOI: 10.4208/aamm.OA-2023-0186
February 2026

Pointwise Goal-Oriented a Posteriori Error Estimates Using Dual Problems with Dirac Delta Source Terms for Linear Elliptic Problems

Fei Li[1,2], Jingang Liu[4], Nianyu Yi[1,3,4] and Liuqiang Zhong[2,*]

[1] *School of Mathematics and Computational Science, Xiangtan University, Xiangtan, Hunan 411105, China*

[2] *School of Mathematical Sciences, South China Normal University, Guangzhou, Guangdong 510631, China*

[3] *Hunan Key Laboratory for Computation and Simulation in Science and Engineering, School of Mathematics and Computational Science, Xiangtan University, Xiangtan, Hunan 411105, China*

[4] *Hunan National Center for Applied Mathematics, Xiangtan, Hunan 411105, China*

Received 11 July 2023; Accepted (in revised version) 20 February 2024

Abstract. In this paper, a pointwise goal-oriented residual-based a posteriori error estimator is proposed for linear elliptic equations with restricted source terms. The pointwise error is directly estimated by introducing the dual problem with a Dirac delta source term instead of using classical mollification technique. The goal-oriented error estimator is proved to be the upper bound of the pointwise error. Numerical experiments show the advantage of the adaptive finite element method (AFEM) based on this error estimator, which can preserve the monotonicity of the pointwise error, compared with the goal-oriented AFEM using the mollification technique.

AMS subject classifications: 65M10, 78A48

Key words: Pointwise quantity of interest, a posteriori error estimate, adaptive finite element method, Dirac delta source term.

1 Introduction

Goal-oriented a posteriori error estimates have been widely attentioned in the past of more than two decades, and have been applied in many fields, such as elasticity [24, 30], hydromechanics [10, 16, 20], and electromagnetism [8, 21]. In contrast to a posteriori

*Corresponding author.
Email: lifeimath@scnu.edu.cn (F. Li), liujingang@xtu.edu.cn (J. Liu), yinianyu@xtu.edu.cn (N. Yi), zhong@scnu.edu.cn (L. Zhong)

error estimates [1, 31] that normally assess errors in the global energy norm, the goal-oriented a posteriori error estimates [5, 23, 26, 27, 32] evaluate errors of the specific goals, which are quantified as functional values of the solution of the problem. The functional values generally represent physical quantities of practical interest [4, 6, 15], and therefore, the goal-oriented a posteriori error estimate is usually more important in practice than the normal a posteriori error estimate. This paper focuses on the pointwise quantity of interest, i.e., the value of the solution at a point of interest in the physical domain, e.g., the temperature at a critical point, one can see [27–29] for the related work on this quantity of interest.

The quantity of interest is generally treated as an integral type of quantity of interest, which is an averaging of the solution over a small neighborhood of the point of interest, since the point value of the solution being a function in Sobolev spaces may not be well defined, i.e., the solution is discontinuous at the point of interest. This treatment is called mollification technique [27,28]. However, if the pointwise quantity of interest can be well defined, the goal-oriented a posteriori error estimate using the mollification technique does not assess the pointwise error but the error in another integral-averaging quantity of interest. Numerical experiments show that, for some model problems, this error estimate leads to that the pointwise error is not monotone-decreasing on the generating adaptive mesh sequence, which is unexpected (see Figs. 5 and 8 in Section 4).

The pointwise error estimation in this paper is different from the one using the mollification technique, and introduces a dual problem with the Dirac delta source term to directly estimate the pointwise error. We construct a theoretically reliable pointwise goal-oriented a posteriori error estimator, and numerical experiments indicate the advantage of the adaptive finite element method (AFEM) based on this error estimator that, for some model problems, it can preserve the monotone-decreasing behavior of the pointwise error, while the pointwise goal-oriented AFEM using the mollification technique cannot.

The structure of this paper is as follows: In Section 2, we present the primal model problem and the dual problem involved in their continuous, variational and discretization forms, and derive the error estimate in the pointwise quantity of interest. In Section 3, we define the primal, the dual, and the goal-oriented a posteriori error estimators, and prove their reliability. Section 3 ends up with formulating the adaptive finite element algorithm based on the pointwise goal-oriented error estimator. In Section 4, numerical experiments show the validity and advantage of the proposed algorithm.

2 Preliminaries

First, we introduce some notations with respect to spaces and norms. Given $D \subset \mathbb{R}^2$, let

$$L^r(D) := \{v \in L^1(D) : \|v\|_{0,r,D} < \infty\}, \quad 1 \le r \le \infty,$$

where $L^1(D)$ denotes the standard Lebesgue space on D, and the associated norm

$$\|v\|_{0,r,D}=\begin{cases}\left(\int_D |v|^r \mathrm{d}\boldsymbol{x}\right)^{\frac{1}{r}}, & 1\le r<\infty,\\ \operatorname{ess\,sup}_{\boldsymbol{x}\in D}|v(\boldsymbol{x})|, & r=\infty.\end{cases}$$

The Sobolev space $W^{1,r}(D)$ consists of functions belonging to $L^r(D)$ whose first-order distributional derivative also belongs to $L^r(D)$, and it is equipped with the norm $\|v\|_{1,r,D}=\|v\|_{0,r,D}+|v|_{1,r,D}$ for $v\in W^{1,r}(D)$, where $|v|_{1,r,D}=\|\nabla v\|_{0,r,D}$ signifies the $W^{1,r}$-seminorm. Especially, $W^{1,2}(D)=:H^1(D)$. Note that we simplify the norm $\|\cdot\|_{0,2,D}=\|\cdot\|_{0,D}$, and if D is the domain where the model problem is defined, the subscript of domain in norms is omitted. In addition, $\mathcal{C}(D)$ denotes the continuous function space on D.

We consider the following linear elliptic problem

$$-\operatorname{div}(a\nabla u)=f \qquad \text{in } \Omega, \tag{2.1a}$$

$$u=g \qquad \text{on } \partial\Omega, \tag{2.1b}$$

where $\Omega\in\mathbb{R}^2$ is a bounded Lipschitz domain with boundary $\partial\Omega$, the matrix $a:\Omega\to\mathbb{R}^{2\times 2}$ is Lipschitz continuous, symmetric and positive-definite such that

$$\inf_{\boldsymbol{x}\in\Omega}\lambda_{\min}(a(\boldsymbol{x}))=\mu_0>0, \quad \sup_{\boldsymbol{x}\in\Omega}\lambda_{\max}(a(\boldsymbol{x}))=\mu_1<\infty, \tag{2.2}$$

in which $\lambda_{\min}$ and $\lambda_{\max}$ denote the minimum and maximum eigenvalues of $a(\boldsymbol{x})$, the source term f is restricted in $L^q(\Omega)$ with $2<q<\infty$, which implies that $u\in W^{1,q}(\Omega)$ from elliptic regularity theory [11], and the Dirichlet boundary condition $g\in L^q(\partial\Omega)$. By the homogeneous principle, we can obtain the homogeneous Dirichlet boundary condition. For ease of presentation, assume $g=0$.

Let $W_0^{1,q}(\Omega):=\{v\in W^{1,q}(\Omega):v|_{\partial\Omega}=0\}$. The variational formulation of problem (2.1a)–(2.1b) reads: Find $u\in W_0^{1,q}(\Omega)$ such that

$$(a\nabla u,\nabla v)=(f,v), \quad \forall v\in W_0^{1,p}(\Omega), \tag{2.3}$$

where $2<q<\infty$ and $1<p<2$ such that $\frac{1}{p}+\frac{1}{q}=1$, and $(v,w)_D=\int_D vw\mathrm{d}\boldsymbol{x}$, especially, $(v,w)=(v,w)_\Omega$.

Throughout this paper, we are interested in the value of the solution u of problem (2.1a)–(2.1b) at a given point $\boldsymbol{x}_1\in\Omega$, i.e., consider the following pointwise quantity of interest

$$Q_{\boldsymbol{x}_1}(u)=u(\boldsymbol{x}_1). \tag{2.4}$$

Thank to the solution $u\in W^{1,q}(\Omega)\subset\mathcal{C}(\Omega)$, $2<q<\infty$ from the inclusion relation of Sobolev spaces [7,13], the quantity of interest $Q_{\boldsymbol{x}_1}(u)$ is well defined.

By means of the property of the Dirac delta function, we obtain

$$Q_{\boldsymbol{x}_1}(u)=u(\boldsymbol{x}_1)=\int_\Omega \delta_{\boldsymbol{x}_1}(\boldsymbol{x})u(\boldsymbol{x})\mathrm{d}\boldsymbol{x}, \tag{2.5}$$

where $\delta_{x_1}=\delta(\boldsymbol{x}-\boldsymbol{x}_1)$. To estimate the error in the quantity of interest $Q_{x_1}(u)$, based on the identity (2.5), we define a continuous dual problem with the Dirac delta source term:

$$-\mathrm{div}(a\nabla z)=\delta_{x_1} \qquad \text{in } \Omega, \tag{2.6a}$$

$$z=0 \qquad \text{on } \partial\Omega, \tag{2.6b}$$

whose corresponding variational formulation reads: Find $z\in W_0^{1,p}(\Omega)$ such that

$$(a\nabla w,\nabla z)=Q_{x_1}(w), \quad \forall w\in W_0^{1,q}(\Omega). \tag{2.7}$$

Remark 2.1. For the case that a is the identity matrix in (2.1a), from [3], we know the fundamental solution

$$G=-\frac{1}{2\pi}\log|\boldsymbol{x}-\boldsymbol{x}_1| \quad \text{satisfies } -\Delta G=\delta_{x_1},$$

where $G\in W^{1,p}(\Omega)$ with arbitrary $1<p<2$. According to the superposition principle, the solution of (2.6a)–(2.6b), $z=G+\tilde{z}$, where $\tilde{z}$ is determined by

$$-\Delta\tilde{z}=0 \qquad \text{in } \Omega,$$

$$\tilde{z}=-G \qquad \text{on } \partial\Omega.$$

Note that $\boldsymbol{x}_1\in\Omega$, then G is continuous on $\partial\Omega$ and $\tilde{z}\in H^1(\Omega)$. Therefore, $z=G+\tilde{z}\in W_0^{1,p}(\Omega)$ for arbitrary $1<p<2$.

For more work with respect to finite element methods of elliptic problems with the Dirac delta source terms, one can refer to [2,3,19,22].

Let $\mathcal{T}_h$ be an admissible and shape-regular triangulation of Ω. For simplicity, assume that the point of interest $\boldsymbol{x}_1$ is a vertex of $\mathcal{T}_h$. We denote by h_T and h_e the sizes of any triangle element $T\in\mathcal{T}_h$ and any edge $e\in\mathcal{E}_h^i$, respectively, where $\mathcal{E}_h^i$ is the set of all interior edges in triangulation $\mathcal{T}_h$. The shape regularity of the triangulation implies $h_T\simeq h_e$. Let $h:=\max_{T\in\mathcal{T}_h}h_T$. Define the continuous piecewise linear finite element space associated with triangulation $\mathcal{T}_h$ as follows:

$$\mathbb{V}_h:=\{v_h\in\mathcal{C}(\Omega):v_h|_T\in\mathbb{P}_1(T),\ T\in\mathcal{T}_h\},$$

where $\mathbb{P}_1(T)$ consists of all linear polynomials on T. Let $\mathbb{V}_h^0:=\{v_h\in\mathbb{V}_h:v_h|_{\partial\Omega}=0\}$. Note that $\mathbb{V}_h^0\subset W_0^{1,q}(\Omega)\subset W_0^{1,p}(\Omega)$ with $1<p<2$ and $2<q<\infty$ satisfying $\frac{1}{p}+\frac{1}{q}=1$.

The finite element discretization of the primal problem (2.1a)–(2.1b) reads: Find $u_h\in\mathbb{V}_h^0$ such that

$$(a\nabla u_h,\nabla v_h)=(f,v_h), \quad \forall v_h\in\mathbb{V}_h^0, \tag{2.8}$$

and the finite element discretization of the dual problem (2.6a)–(2.6b) reads: Find $z_h\in\mathbb{V}_h^0$ such that

$$(a\nabla w_h,\nabla z_h)=Q_{x_1}(w_h), \quad \forall w_h\in\mathbb{V}_h^0. \tag{2.9}$$

Taking $w=u-u_h\in W_0^{1,q}(\Omega)$ in the variational dual problem (2.7), and using the following orthogonality relation for the primal problem

$$(a\nabla(u-u_h),\nabla v_h)=0,\quad \forall v_h\in\mathbb{V}_h^0, \tag{2.10}$$

yield the error representation and estimate for the pointwise quantity of interest

$$\begin{aligned}Q_{x_1}(u)-Q_{x_1}(u_h)=&Q_{x_1}(u-u_h)=(a\nabla(u-u_h),\nabla z)\\ =&(a\nabla(u-u_h),\nabla(z-z_h))\\ \le&\|a^{\frac{1}{q}}\nabla(u-u_h)\|_{0,q}\|a^{\frac{1}{p}}\nabla(z-z_h)\|_{0,p}.\end{aligned} \tag{2.11}$$

Remark 2.2. The estimation for the pointwise error usually utilizes the mollification technique [28], which can deal with the case that the point value of the primal solution in Sobolev spaces may not be well defined, i.e., is discontinuous at the point of interest. For the pointwise quantity of interest $u(\boldsymbol{x}_1)$, the mollification technique considers it as an averaging of u over a small neighborhood centered at $\boldsymbol{x}_1$. Introduce another quantity of interest

$$Q_{x_1,\epsilon}(u):=\int_\Omega k_\epsilon(\boldsymbol{x}-\boldsymbol{x}_1)u(\boldsymbol{x})\mathrm{d}\boldsymbol{x}, \tag{2.12}$$

where k_ϵ is called the mollifier, whose normal expression is

$$k_\epsilon(\boldsymbol{x})=\begin{cases}C_\epsilon\exp\Big(-\dfrac{\epsilon^2}{\epsilon^2-|\boldsymbol{x}|^2}\Big), & |\boldsymbol{x}|<\epsilon,\\ 0, & |\boldsymbol{x}|\ge\epsilon,\end{cases} \tag{2.13}$$

here, the constant C_ϵ is determined by

$$\int_\Omega k_\epsilon(\boldsymbol{x}-\boldsymbol{x}_1)\mathrm{d}\boldsymbol{x}=1.$$

Obviously, the mollifier $k_\epsilon(\boldsymbol{x})$ is infinitely continuously differentiable. For $Q_{x_1,\epsilon}(u)$, we define the continuous dual problem

$$-\mathrm{div}(a\nabla\bar{z})=k_\epsilon(\boldsymbol{x}-\boldsymbol{x}_1) \quad \text{in } \Omega, \tag{2.14a}$$

$$\bar{z}=0 \quad \text{on } \partial\Omega. \tag{2.14b}$$

Its variational formulation and the finite element discretization read: Find $\bar{z}\in H_0^1(\Omega)$ such that

$$(a\nabla w,\nabla\bar{z})=Q_{x_1,\epsilon}(w),\quad \forall w\in H_0^1(\Omega),$$

and find $\bar{z}_h\in\mathbb{V}_h^0$ such that

$$(a\nabla w_h,\nabla\bar{z}_h)=Q_{x_1,\epsilon}(w_h),\quad \forall w_h\in\mathbb{V}_h^0,$$

respectively. We readily derive the error representation and estimate for $Q_{x_1,\epsilon}(u)$:

$$\begin{aligned}&Q_{x_1,\epsilon}(u)-Q_{x_1,\epsilon}(u_h)=Q_{x_1,\epsilon}(u-u_h)\\=&(a\nabla(u-u_h),\nabla\bar{z})\\=&(a\nabla(u-u_h),\nabla(\bar{z}-\bar{z}_h))\\\leq&\|a^{\frac{1}{2}}\nabla(u-u_h)\|_0\|a^{\frac{1}{2}}\nabla(\bar{z}-\bar{z}_h)\|_0.\end{aligned}\tag{2.15}$$

The corresponding a posteriori error estimator can be constructed by the product of the standard residual-based a posteriori error estimator for errors $\|a^{\frac{1}{2}}\nabla(u-u_h)\|_0$ and $\|a^{\frac{1}{2}}\nabla(\bar{z}-\bar{z}_h)\|_0$.

The solution $u\in H_0^1(\Omega)$, namely, the source term $f\in L^2(\Omega)$ suffices for the above error estimation based on the mollification technique, this is the general case. However, for the special case that u is continuous at the point of interest $\boldsymbol{x}_1$, namely, the quantity of interest $Q_{x_1}(u)=u(\boldsymbol{x}_1)$ is well defined, the error estimation based on the mollification technique indeed estimates the error $|Q_{x_1,\epsilon}(u)-Q_{x_1,\epsilon}(u_h)|$ rather than the point error $|u(\boldsymbol{x}_1)-u_h(\boldsymbol{x}_1)|$. Numerical experiments reflect that the adaptive algorithm based on this error estimate leads to that the pointwise error exhibits the unexpected nonmonotonic reduction (see Figs. 5 and 8 in Section 4).

Remark 2.3. Although we restrict the primal source term $f\in L^q(\Omega)$, $q>2$, while the mollification technique only requires $f\in L^2(\Omega)$, note that our method can directly estimate the point error, whereas the mollification technique evaluates the error of (2.12). Furthermore, we numerically compare the proposed method, Algorithm 3.1 below, and the goal-oriented adaptive method based on the mollification technique in Example 4.2 of Section 4. This comparison highlights that the point error of the proposed algorithm can maintain monotone-decreasing but the classical one cannot.

Suppose that the support of the mollifier $k_\epsilon(\boldsymbol{x}-\boldsymbol{x}_1)$ is always inside Ω for any $\epsilon>0$. From [28] we know two cases with respect to the asymptotics between the averaging quantity of interest $Q_{x_1,\epsilon}(u)$ and the pointwise one $Q_{x_1}(u)=u(\boldsymbol{x}_1)$: one is that $Q_{x_1,\epsilon}(u)=Q_{x_1}(u)$ holds for each value of ϵ whenever the primal solution u is constant or linear in Ω; the other is that $Q_{x_1,\epsilon}(u)$ converges to $Q_{x_1}(u)$ as ϵ tends to zero provided that the primal solution u is continuous in the neighborhood of $\boldsymbol{x}_1$.

3 A posteriori error estimate and adaptive algorithm

In this section, we first define the residual-type a posteriori estimators of $\|a^{\frac{1}{q}}\nabla(u-u_h)\|_{0,q}$ and $\|a^{\frac{1}{p}}\nabla(z-z_h)\|_{0,p}$, and prove their reliability. Then, based on the error estimate (2.11), we use the product of the primal and dual error estimators as the goal-oriented a posteriori error estimator being the upper bound of $|Q_{x_1}(u)-Q_{x_1}(u_h)|$. Finally, for goal-oriented adaptivity, we discuss the marking strategy and formulate the goal-oriented adaptive finite element algorithm.

For any element $T\in\mathcal{T}_h$ and any edge $e\in\mathcal{E}_h^i$, define the residuals and the interior edge jump

$$\begin{aligned}&R_T(u_h):=f+\operatorname{div}(a\nabla u_h),\\&R_T^*(z_h):=\operatorname{div}(a\nabla z_h),\\&J_e(v):=[a\nabla v]_e=\big(a\nabla v|_{\partial T_1\cap e}-a\nabla v|_{\partial T_2\cap e}\big)\cdot\boldsymbol{n}_{12},\end{aligned}$$

where $T_1,T_2\in\mathcal{T}_h$ are two neighboring elements sharing with a common edge $e\in\mathcal{E}_h^i$, and $\boldsymbol{n}_{12}$ represents the unit normal vector pointing from T_1 to T_2.

By means of those notations, define the local primal and dual a posteriori error estimators as follows:

$$\eta_{q,h}(T):=\Big(h_T^q\|R_T(u_h)\|_{0,q,T}^q+\sum_{e\subset\partial T\setminus\partial\Omega}h_e\|J_e(u_h)\|_{0,q,e}^q\Big)^{1/q},\tag{3.1a}$$

$$\zeta_{p,h}(T):=\Big(h_T^p\|R_T^*(z_h)\|_{0,p,T}^p+\sum_{e\subset\partial T\setminus\partial\Omega}h_e\|J_e(z_h)\|_{0,p,e}^p\Big)^{1/p},\tag{3.1b}$$

with $2<q<\infty$ and $1<p<2$ satisfying $\frac{1}{p}+\frac{1}{q}=1$. The global analogs are denoted by

$$\eta_{q,h}=\Big(\sum_{T\in\mathcal{T}_h}\eta_{q,h}^q(T)\Big)^{1/q},\quad\zeta_{p,h}=\Big(\sum_{T\in\mathcal{T}_h}\zeta_{p,h}^p(T)\Big)^{1/p}.\tag{3.2}$$

Before proving the reliability of the primal and dual error estimators $\eta_{q,h}$ and $\zeta_{p,h}$, we introduce some essential interpolants and auxiliary problems.

Lemma 3.1 ([3,31]). *There exists a quasi-interpolation operator $\mathcal{I}_h:W^{1,r}(\Omega)\to\mathbb{V}_h$, $1<r<\infty$, such that for any function $v\in W^{1,r}(\Omega)$, any element $T\in\mathcal{T}_h$ and any edge $e\in\mathcal{E}_h^i$, these local approximation properties hold*

$$\|v-\mathcal{I}_hv\|_{0,r,T}\lesssim h_T\|\nabla v\|_{0,r,\tilde{\omega}_T},\tag{3.3a}$$

$$\|v-\mathcal{I}_hv\|_{0,r,e}\lesssim h_e^{1-1/r}\|\nabla v\|_{0,r,\tilde{\omega}_e},\tag{3.3b}$$

where $\lesssim$ denotes $\leq$ up to a generic multiplicative constant $C>0$ which may be different in different place, but independent of the mesh size h, and

$$\tilde{\omega}_T:=\{T'\in\mathcal{T}_h:\overline{T'}\cap\overline{T}\neq\emptyset\},\quad\tilde{\omega}_e:=\{T'\in\mathcal{T}_h:\overline{T'}\cap e\neq\emptyset\}.$$

Furthermore, for the Lagrange interpolation operator $\mathcal{L}_h:\mathcal{C}(\Omega)\to\mathbb{V}_h$, the following approximation properties hold

$$\|v-\mathcal{L}_hv\|_{0,r,T}\lesssim h_T\|\nabla v\|_{0,r,T},\tag{3.4}$$

$$\|v-\mathcal{L}_hv\|_{0,r,e}\lesssim h_e^{1-1/r}\|\nabla v\|_{0,r,\omega_e},\tag{3.5}$$

for any $v\in W^{1,r}(\Omega),2<r<\infty$, where $\omega_e:=\{T\in\mathcal{T}_h:\partial T\supset e\}$.

As in [3], for given $\boldsymbol{\Phi}\in\boldsymbol{L}^r(\Omega)^2$ with $1<r<\infty$, we can define the following auxiliary problem: Find $\phi\in W_0^{1,r}(\Omega)$ such that

$$(a\nabla\phi,\nabla\psi)=(\boldsymbol{\Phi},a^{\frac{1}{t}}\nabla\psi),\quad \forall\psi\in W_0^{1,t}(\Omega), \tag{3.6}$$

where t satisfies $\frac{1}{r}+\frac{1}{t}=1$. The well-posedness of (3.6) and the regularity estimate

$$\|a^{\frac{1}{r}}\nabla\phi\|_{0,r}\lesssim\|\boldsymbol{\Phi}\|_{0,r} \tag{3.7}$$

hold for $1<r<\infty$, namely, $1<t<\infty$, if Ω is convex, or

$$1<r<\frac{2}{1-\frac{\pi}{\vartheta}},\quad \text{namely,}\quad \frac{2}{1+\frac{\pi}{\vartheta}}<t<\infty,$$

if Ω is nonconvex, where ϑ is the largest inner angle of a polygonal domain Ω.

Theorem 3.1 (Reliability of $\eta_{q,h}$ and $\zeta_{p,h}$)**.** *For $2<q<q^\Omega$ and $p^\Omega<p<2$ such that $\frac{1}{p}+\frac{1}{q}=1$, where*

$$p^\Omega:=\max\left\{1,\frac{2}{1+\frac{\pi}{\vartheta}}\right\},\quad q^\Omega:=\begin{cases}\infty, & \Omega\ \textit{is convex},\\ \dfrac{2}{1-\frac{\pi}{\vartheta}}, & \Omega\ \textit{is nonconvex},\end{cases}$$

there hold

$$\|a^{\frac{1}{q}}\nabla(u-u_h)\|_{0,q}\lesssim\eta_{q,h}, \tag{3.8a}$$

$$\|a^{\frac{1}{p}}\nabla(z-z_h)\|_{0,p}\lesssim\zeta_{p,h}. \tag{3.8b}$$

Proof. Given $\boldsymbol{\Phi}\in L^{q'}(\Omega)^2$ with $1<q'<2$, then take $r=q'\in(1,2)\subset(1,4)\subset(1,q^\Omega)$ in (3.6), namely, $t=q\in(2,\infty)$ satisfying $\frac{1}{q'}+\frac{1}{q}=1$, and $\phi\in W_0^{1,q'}(\Omega)$ is the solution of (3.6). Noticing $u-u_h\in W_0^{1,q}(\Omega)$, taking the test function $\psi=u-u_h$ in (3.6), and applying the orthogonality relation (2.10) for the primal problem with $v_h=\mathcal{I}_h\phi$ and the integration by parts, we see that

$$\begin{aligned}&(a^{\frac{1}{q}}\nabla(u-u_h),\boldsymbol{\Phi})=(a\nabla(u-u_h),\nabla\phi)\\ =&(a\nabla(u-u_h),\nabla(\phi-\mathcal{I}_h\phi))=(f,\phi-\mathcal{I}_h\phi)-(a\nabla u_h,\nabla(\phi-\mathcal{I}_h\phi))\\ =&\sum_{T\in\mathcal{T}_h}\int_T R_T(u_h)(\phi-\mathcal{I}_h\phi)\mathrm{d}\boldsymbol{x}-\sum_{e\in\mathcal{E}_h^i}\int_e J_e(u_h)(\phi-\mathcal{I}_h\phi)\mathrm{d}s.\end{aligned} \tag{3.9}$$

Using the Hölder inequality, the local approximation properties (3.3a) and (3.3b) of oper-

ator $\mathcal{I}_h$ and the Cauchy-Schwarz inequality yields

$$\begin{aligned}(a^{\frac{1}{q}}\nabla(u-u_h),\boldsymbol{\Phi}) &\leq \sum_{T\in\mathcal{T}_h}\|R_T(u_h)\|_{0,q,T}\|\phi-\mathcal{I}_h\phi\|_{0,q',T}+\sum_{e\in\mathcal{E}_h^i}\|J_e(u_h)\|_{0,q,e}\|\phi-\mathcal{I}_h\phi\|_{0,q',e}\\ &\lesssim \sum_{T\in\mathcal{T}_h}\|R_T(u_h)\|_{0,q,T}\,h_T\|\nabla\phi\|_{0,q',\tilde{\omega}_T}+\sum_{e\in\mathcal{E}_h^i}\|J_e(u_h)\|_{0,q,e}\,h_e^{1-\frac{1}{q'}}\|\nabla\phi\|_{0,q',\tilde{\omega}_e}\\ &\lesssim\Big(\sum_{T\in\mathcal{T}_h}h_T^q\|R_T(u_h)\|_{0,q,T}^q+\sum_{e\in\mathcal{E}_h^i}h_e\|J_e(u_h)\|_{0,q,e}^q\Big)^{1/q}\\ &\quad\cdot\Big(\sum_{T\in\mathcal{T}_h}\|\nabla\phi\|_{0,q',\tilde{\omega}_T}^{q'}+\sum_{e\in\mathcal{E}_h^i}\|\nabla\phi\|_{0,q',\tilde{\omega}_e}^{q'}\Big)^{1/q'}\\ &\lesssim\eta_{q,h}\|\boldsymbol{\Phi}\|_{0,q'},\end{aligned}\tag{3.10}$$

where the shape regularity of triangulation $\mathcal{T}_h$, the condition (2.2) on the matrix a and the regularity estimate (3.7) with $r=q'$ imply that

$$\Big(\sum_{T\in\mathcal{T}_h}\|\nabla\phi\|_{0,q',\tilde{\omega}_T}^{q'}+\sum_{e\in\mathcal{E}_h^i}\|\nabla\phi\|_{0,q',\tilde{\omega}_e}^{q'}\Big)^{1/q'}\lesssim\|\nabla\phi\|_{0,q'}\lesssim\|a^{\frac{1}{q'}}\nabla\phi\|_{0,q'}\lesssim\|\boldsymbol{\Phi}\|_{0,q'}.$$

Therefore, we conclude that

$$\|a^{\frac{1}{q}}\nabla(u-u_h)\|_{0,q}=\sup_{\boldsymbol{\Phi}\in L^{q'}(\Omega)^2\setminus\{0\}}\frac{(a^{\frac{1}{q}}\nabla(u-u_h),\boldsymbol{\Phi})}{\|\boldsymbol{\Phi}\|_{0,q'}}\lesssim\eta_{q,h}.$$

Reset $\boldsymbol{\Phi}\in L^{p'}(\Omega)^2$ with $1<p'<q^\Omega$, then take $r=p'$ in (3.6), namely, $p\in(p^\Omega,\infty)\cap(1,2)=(p^\Omega,2)$ satisfying $\frac{1}{p'}+\frac{1}{p}=1$, hence the relation $\frac{1}{q}+\frac{1}{p}=1$ implies that $q\in(2,q^\Omega)$. At this time, (3.6) admits the solution $\phi\in W_0^{1,p'}(\Omega)\subset\mathcal{C}(\Omega)$ due to $p'=q$, and note that $z-z_h\in W_0^{1,p}(\Omega)$. Analogously, we obtain

$$\begin{aligned}&(a^{\frac{1}{p}}\nabla(z-z_h),\boldsymbol{\Phi})=(a\nabla(z-z_h),\nabla\phi)\\ &=(a\nabla(z-z_h),\nabla(\phi-\mathcal{L}_h\phi))\\ &=(\delta_{\boldsymbol{x}_1},\phi-\mathcal{L}_h\phi)-(a\nabla z_h,\nabla(\phi-\mathcal{L}_h\phi))\qquad(3.11)\\ &=\sum_{T\in\mathcal{T}_h}\int_T R_T^*(z_h)(\phi-\mathcal{L}_h\phi)\mathrm{d}\boldsymbol{x}-\sum_{e\in\mathcal{E}_h^i}\int_e J_e(z_h)(\phi-\mathcal{L}_h\phi)\mathrm{d}s,\qquad(3.12)\end{aligned}$$

where $(\delta_{\boldsymbol{x}_1},\phi-\mathcal{L}_h\phi)=(\phi-\mathcal{L}_h\phi)(\boldsymbol{x}_1)=0$ since $\mathcal{L}_h$ is a Lagrange interpolation operator. Furthermore, similar to the derivation of the result (3.10), we show that

$$(a^{\frac{1}{p}}\nabla(z-z_h),\boldsymbol{\Phi})\lesssim\zeta_{p,h}\|\boldsymbol{\Phi}\|_{0,p'}.$$

We also conclude that

$$\|a^{\frac{1}{p}}\nabla(z-z_h)\|_{0,p}=\sup_{\mathbf{\Phi}\in L^{p'}(\Omega)^2\setminus\{0\}}\frac{(a^{\frac{1}{p}}\nabla(z-z_h),\mathbf{\Phi})}{\|\mathbf{\Phi}\|_{0,p'}}\lesssim\zeta_{p,h}.$$

This completes the proof. □

Remark 3.1. If the point of interest $\boldsymbol{x}_1$ is not a vertex for a given mesh, i.e., $\boldsymbol{x}_1$ belongs to an element $\hat{T}$, then the local dual error estimator only associated with the element $\hat{T}$ needs to be redefined by

$$\zeta_{p,h}(\hat{T}):=\Big(h_{\hat{T}}^{2-p}+h_{\hat{T}}^{p}\|R_{\hat{T}}^{*}(z_h)\|_{0,p,\hat{T}}^{p}+\sum_{e\subset\partial\hat{T}\setminus\partial\Omega}h_e\|J_e(z_h)\|_{0,p,e}^{p}\Big)^{1/p}.$$

Note that the term $(\delta_{\boldsymbol{x}_1},\phi-\mathcal{L}_h\phi)=(\phi-\mathcal{L}_h\phi)(\boldsymbol{x}_1)\neq 0$ in (3.11). By means of the standard interpolation error estimate (e.g., [9]) and $\frac{1}{p}+\frac{1}{p'}=1$, it follows that

$$(\delta_{\boldsymbol{x}_1},\phi-\mathcal{L}_h\phi)\leq\|\phi-\mathcal{L}_h\phi\|_{0,\infty,\hat{T}}\leq h_{\hat{T}}^{1-2/p'}\|\nabla\phi\|_{0,p',\hat{T}}=h_{\hat{T}}^{(2-p)/p}\|\nabla\phi\|_{0,p',\hat{T}}.$$

Consider the estimator product $\eta_{q,h}\zeta_{p,h}$ as the a posteriori error estimator for the pointwise quantity of interest $Q_{\boldsymbol{x}_1}(u)=u(\boldsymbol{x}_1)$. Applying results (3.8a) and (3.8b) of Theorem 3.1 to (2.11) immediately yields the following corollary.

Corollary 3.1 (Reliability of goal-oriented a posteriori error estimator)**.** *Under the conditions of Theorem* 3.1*, it holds*

$$|Q_{\boldsymbol{x}_1}(u)-Q_{\boldsymbol{x}_1}(u_h)|=|u(\boldsymbol{x}_1)-u_h(\boldsymbol{x}_1)|\lesssim\eta_{q,h}\zeta_{p,h}. \tag{3.13}$$

Remark 3.2. As mentioned in Section 1.11 of [31], for a general linear functional, one cannot expect the efficiency of the goal-oriented a posteriori error estimator since $u-u_h$ may be in the kernel of the goal functional. In some references [12,25] in which the enriched finite element approximations and a related saturation assumption on the quantity of interest are used, the efficiency of the goal-oriented error estimator can be proved. In our numerical results, particularly, Fig. 8a shows a perfect match between the goal-oriented error estimator and the real point error. The efficiency could be a good interpretation for this phenomenon, but its proof is an open problem.

In the following, we discuss the marking strategy for goal-oriented adaptivity. Adaptive finite element methods normally use the Dörfler marking in sense of the ℓ^2-norm. The goal-oriented adaptive finite element methods proposed by [17,18] apply the Dörfler marking in sense of the ℓ^2-norm to primal and dual error estimators, respectively, and take the union of their marking sets as the final marking set. This can largely capture the singularities on the primal and dual solutions simultaneously.

However, for error estimators $\eta_{q,h}$ and $\zeta_{p,h}$ defined in (3.2), it is worth emphasizing that we adopt the Dörfler marking in sense of the ℓ^q-norm for $\eta_{q,h}$ and the ℓ^p-norm for $\zeta_{p,h}$, i.e., find two sets $\mathcal{M}_1$ and $\mathcal{M}_2$ of the minimal cardinality such that

$$\sum_{T\in\mathcal{M}_1}\eta_{q,h}^q(T)\geq\theta\eta_{q,h}^q,\quad \sum_{T\in\mathcal{M}_2}\zeta_{p,h}^p(T)\geq\theta\zeta_{p,h}^p, \tag{3.14}$$

and take $\mathcal{M}_h=\mathcal{M}_1\cup\mathcal{M}_2$, where $\theta\in(0,1)$ is the marking threshold.

Remark 3.3. Note that the error in the quantity of interest is the product of errors of the primal and dual problems, hence it is influenced by singularities on the primal and dual solutions. Obviously, it is not suitable to select $\mathcal{M}_1$ or $\mathcal{M}_2$ as the overall marking set. Except the used overall marking set $\mathcal{M}_h=\mathcal{M}_1\cup\mathcal{M}_2$ (Strategy A), the reference [14] proposed another marking strategy (Strategy B). This strategy picks $\widetilde{\mathcal{M}}_h$ to be the minimal set of $\mathcal{M}_1$ and $\mathcal{M}_2$, and enlarge $\widetilde{\mathcal{M}}_h$ by adding the largest $\#\widetilde{\mathcal{M}}_h$ elements of the other set, as the overall marking set (see Remark 2 of [14]).

From [14,17] one theoretically knows that goal-oriented adaptivity based on Strategy B has higher convergence rate than that based on Strategy A. However, the spaces which the primal and dual solutioins belong to are the same Sobolev spaces (i.e., $p=q=2$) in their works, while in our work, the corresponding spaces are different (i.e., $p\neq q$). Thus, the related convergence proof in our work is an open problem. Note that, in numerical experiments, Fig. 8a suggests that the point error of Algorithm 3.1 (based on Strategy A) stays monotone-decreasing whereas the one of goal-oriented adaptivity based on Strategy B does not. Therefore, we choose Strategy A to design Algorithm 3.1.

We propose adaptive finite element algorithms for the pointwise quantity of interest $Q_{\boldsymbol{x}_1}(u)=u(\boldsymbol{x}_1)$ as follows:

4 Numerical experiment

In this section, we use several numerical tests to illustrate the effectiveness of Algorithm 3.1, and show comparisons between Algorithm 3.1 and the goal-oriented adaptive finite element method based on the mollification technique (see Remark 2.2), to highlight the advantage of Algorithm 3.1.

In the first two examples, we consider the Poisson problem (the matrix a in (2.1a) is the identity matrix) and the analytical solution

$$u_1(\boldsymbol{x})=u_1(x,y)=10e^{-1000((x-0.5)^2+(y-0.5)^2)}, \tag{4.1}$$

defined in a unit square domain $\Omega=(0,1)\times(0,1)$, or

$$u_2(\rho,\xi)=\rho^{\frac{2}{3}}\sin\frac{2}{3}\xi,\quad \rho=\sqrt{x^2+y^2},\quad \xi=\arctan\frac{y}{x}, \tag{4.2}$$

Algorithm 3.1: Adaptive finite element algorithm for pointwise quantity.

Input: An initial triangulation $\mathcal{T}_h$, the values of p and q, the relative error tolerance TOL for the pointwise quantity of interest, the marking threshold $\theta\in(0,1)$ and the increment $n\leftarrow 1$.

Output: The final triangulation, and the approximation and error estimator of the pointwise quantity of interest.

while $n\neq 0$ **do**

Solve the discrete primal problem (2.8) and the discrete dual problem (2.9) on $\mathcal{T}_h$ to obtain the solutions u_h and z_h. Compute the approximation of the quantity of interest $Q_{\boldsymbol{x}_1}(u_h)$;

For each element $T\in\mathcal{T}_h$, compute the local primal and dual a posteriori error estimators $\eta_{q,h}(T)$ and $\zeta_{p,h}(T)$ by (3.1a) and (3.1b), and then calculate the global analogs $\eta_{q,h}$ and $\zeta_{p,h}$ by (3.2). The estimator product $\eta_{q,h}\zeta_{p,h}$ is viewed as the goal-oriented error estimator;

if $\frac{\eta_{q,h}\zeta_{p,h}}{|Q_{\boldsymbol{x}_1}(u_h)|}\leq$ TOL **then**

Return the final triangulatioin $\mathcal{T}_h$, the approximation $Q_{\boldsymbol{x}_1}(u_h)$ and the corresponding error estimator $\eta_{q,h}\zeta_{p,h}$;

The algorithm terminates;

else

Find two sets $\mathcal{M}_1$ and $\mathcal{M}_2$ of the minimal cardinality satisfying the condition (3.14), and let the marking set $\mathcal{M}_h=\mathcal{M}_1\cup\mathcal{M}_2$;

Use the newest vertex bisection to refine $\mathcal{M}_h$ and generate a new triangulation which is still notated by $\mathcal{T}_h$. The increment $n\leftarrow n+1$;

end

end

defined in a L-shaped domain $\Omega=(-1,1)\times(-1,1)\backslash[0,1)\times(-1,0]$. For the solution u_1, we select the point of interest $\boldsymbol{x}_1=(0.5,0.5)$, and for the solution u_2, we choose the point of interest $\boldsymbol{x}_1=(-0.25,0.25)$. In addition, the marking threshold $\theta=0.3$ uniformly.

Example 4.1. This example aims to investigate the behavior of the following effectivity index of the goal-oriented a posteriori error estimator

$$\lambda_{h,q,p}:=\frac{\eta_{q,h}\zeta_{p,h}}{|u(\boldsymbol{x}_1)-u_h(\boldsymbol{x}_1)|},\tag{4.3}$$

with different values of $p\in(1,2)$ (the value q is determined as soon as p is determined). For the analytical solution u_1, select $p=1.1,1.2,\cdots,1.9$, and for u_2, select $p=1.3,1.4,\cdots,1.9$ since $u_2\in W^{1,6-\varepsilon}(\Omega)$ for sufficiently small $\varepsilon>0$, namely, $p\in(1.2,2)$.

Figs. 1 and 2 plot the effectivity index $\lambda_{h,q,p}$ versus the number of mesh vertices N with different values of p for the quantities of interest $Q_{x_1}(u_1)$ and $Q_{x_1}(u_2)$, respectively. From Fig. 1 we see that when $p=1.1,1.2,\cdots,1.7$, the effectivity index $\lambda_{h,q,p}$ is convergent, while $\lambda_{h,q,p}$ with $p=1.8,1.9$ is divergent. From Fig. 2 we observe that the effectivity index $\lambda_{h,q,p}$ only with $p=1.5$ converges, while other values of p make $\lambda_{h,q,p}$ divergent. In conclusion, $p=1.5$ is the optimal choice for both analytical solutions and points of interest.

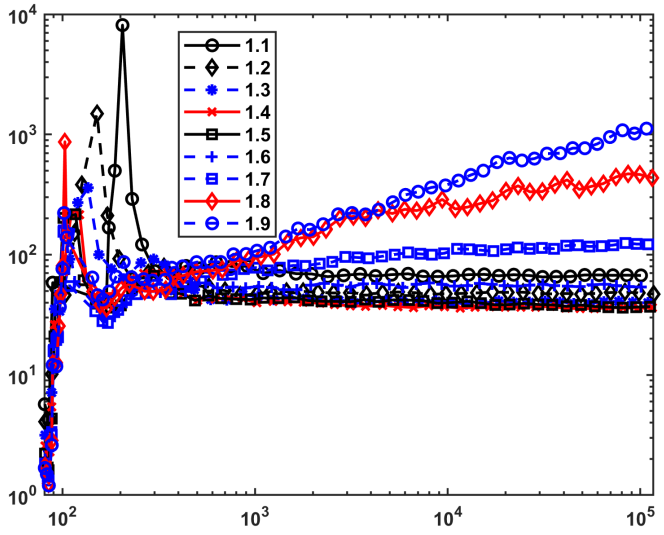

Figure 1: For the pointwise quantity of interest $Q_{x_1}(u_1)$, with different values of p, effectivity index $\lambda_{h,q,p}$ versus the number of mesh vertices N.

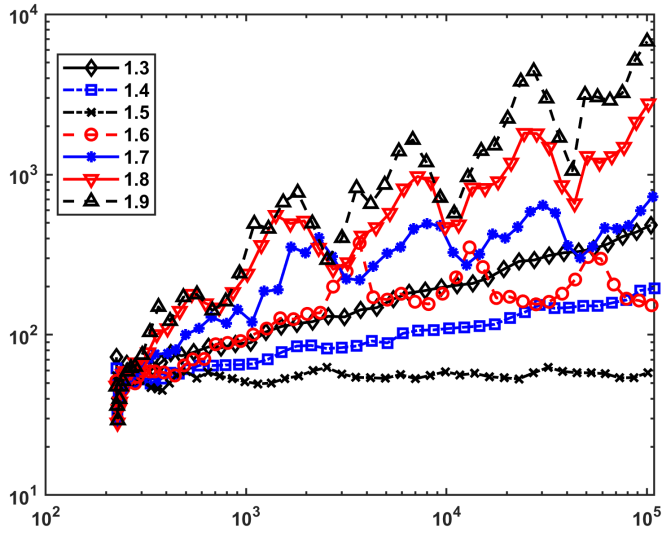

Figure 2: For the pointwise quantity of interest $Q_{x_1}(u_2)$, with different values of p, effectivity index $\lambda_{h,q,p}$ versus the number of mesh vertices N.

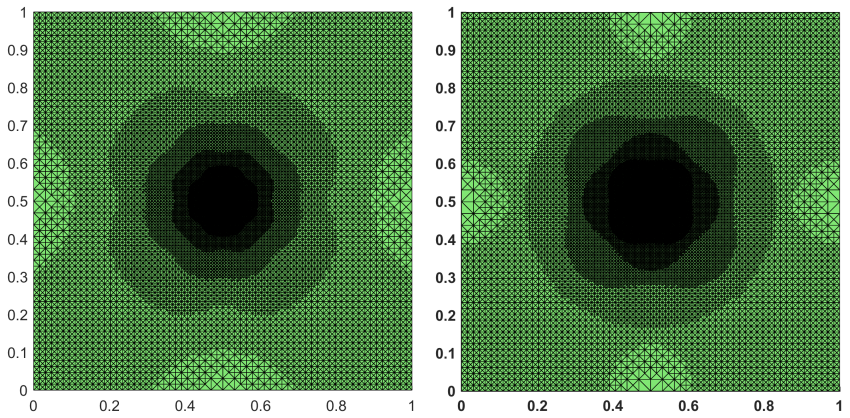

(a) Algorithm 3.1 (b) GOAFEM-MOLL

Figure 3: For the point value $u_1((0.5,0.5))$, adaptive meshes of Algorithm 3.1 and GOAFEM-MOLL.

Example 4.2. We intend to compare Algorithm 3.1 and the goal-oriented adaptive finite element method based on the mollification technique (abbreviated as GOAFEM-MOLL). From Remark 2.2, the goal-oriented a posteriori error estimator of GOAFEM-MOLL can be denoted by the estimator product $\eta_h\zeta_h$, where the primal energy-norm error estimator $\eta_h := \eta_{2,h}$ and the dual energy-norm error estimator ζ_h is defined as

$$\zeta_h := \left(\sum_{T\in\mathcal{T}_h} \left(h_T^2 \| k_\epsilon(\boldsymbol{x}-\boldsymbol{x}_1) + R^*(\bar{z}_h) \|_{0,T}^2 + \sum_{e\subset\partial T\setminus\partial\Omega} h_e \| J_e(\bar{z}_h) \|_{0,e}^2 \right) \right)^{1/2}.$$

In addition, GOAFEM-MOLL uses the marking strategy proposed in [17]. We choose $p=1.5$ for Algorithm 3.1 and $\epsilon = 1/32$ in the quantity of interest $Q_{\boldsymbol{x}_1,\epsilon}(u)$ for GOAFEM-MOLL. For all algorithms, the numerical integration is performed with 7 Gaussian points and the initial mesh size $h_0 = 1/8$.

Figs. 3 and 4 show daptive meshes and the corresponding discrete dual solutions of Algorithm 3.1 and GOAFEM-MOLL for the point value $u_1((0.5,0.5))$. From these results we observe that the mesh refinement for Algorithm 3.1 is more centralized at the point of interest $\boldsymbol{x}_1 = (0.5,0.5)$ than that of GOAFEM-MOLL, and the discrete dual solutions of Algorithm 3.1 is a steep peak, while the one of GOAFEM-MOLL is smoother since the source term $\delta_{\boldsymbol{x}_1}$ in (2.6a) is less regular than the mollifier $k_\epsilon(\boldsymbol{x}-\boldsymbol{x}_1)$ in (2.14a).

Fig. 5 reports errors and the error estimator versus the number of mesh vertices of Algorithm 3.1 and GOAFEM-MOLL for the point value $u_1((0.5,0.5))$. We see that, for Algorithm 3.1, the pointwise error $|u(\boldsymbol{x}_1)-u_h(\boldsymbol{x}_1)|$ and its error estimator $\eta_{q,h}\zeta_{p,h}$ are both monotone-decreasing at the optimal rate, however, for GOAFEM-MOLL, the error $|u(\boldsymbol{x}_1)-u_h(\boldsymbol{x}_1)|$ suggests a nonmonotonic sawtooth reduction, although the quantity of interest based on the mollification $|Q_{\boldsymbol{x}_1,\epsilon}(u)-Q_{\boldsymbol{x}_1,\epsilon}(u_h)|$ and its estimator $\eta_h\zeta_h$ are monotone-decreasing.

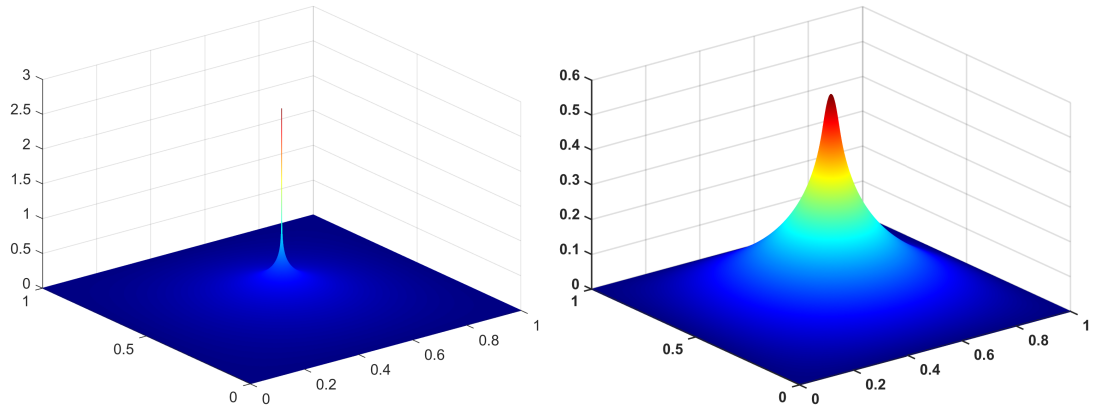

(a) Algorithm 3.1 (b) GOAFEM-MOLL

Figure 4: For the point value $u_1((0.5,0.5))$, discrete dual solutions of Algorithm 3.1 and GOAFEM-MOLL.

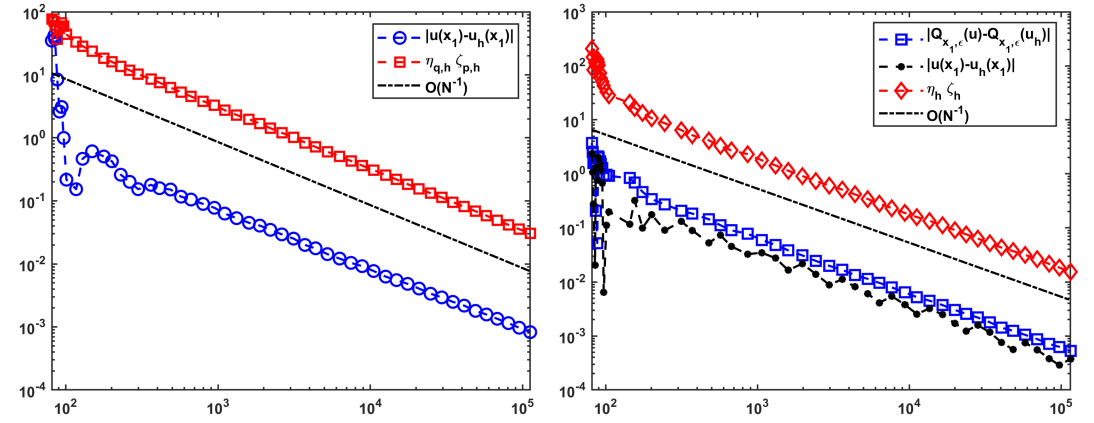

(a) Algorithm 3.1 (b) GOAFEM-MOLL

Figure 5: For point value $u_1((0.5,0.5))$, errors and error estimator versus the number of mesh vertices for Algorithm 3.1 and GOAFEM-MOLL.

Figs. 6 and 7 plot adaptive meshes and the corresponding discrete dual solutions of these two algorithms for $u_2((-0.25,0.25))$. From Fig. 6 we observe that, for Algorithm 3.1, mesh vertices are mainly located in the point of interest, while for GOAFEM-MOLL, mesh vertices are mainly placed in the reentrant corner. This maybe results from the dual solution z of Algorithm 3.1 has stronger singularity than the primal solution u_2, and u_2 has stronger singularity than the dual solution $\bar{z}$ of GOAFEM-MOLL. This leads to that, for Algorithm 3.1, the dual marking set $\mathcal{M}_2$ consists of more elements than the primal marking set $\mathcal{M}_1$, while for GOAFEM-MOLL, it is just the reverse. Moreover, Fig. 7 reflects the similar phenomenon as Fig. 4.

Fig. 8 shows errors and the error estimator versus the number of mesh vertics of Al-

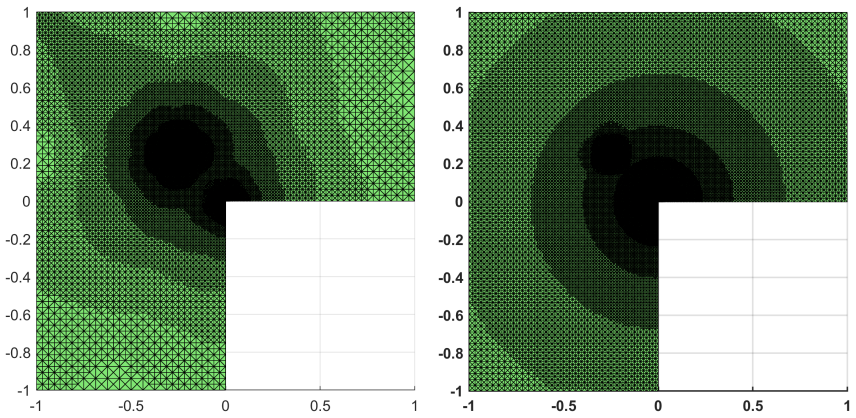

(a) Algorithm 3.1 (b) GOAFEM-MOLL

Figure 6: For the point value $u_2((-0.25,0.25))$, adaptive meshes of Algorithm 3.1 ($\#\mathcal{T}_h$=321164) and GOAFEM-MOLL ($\#\mathcal{T}_h$=30461).

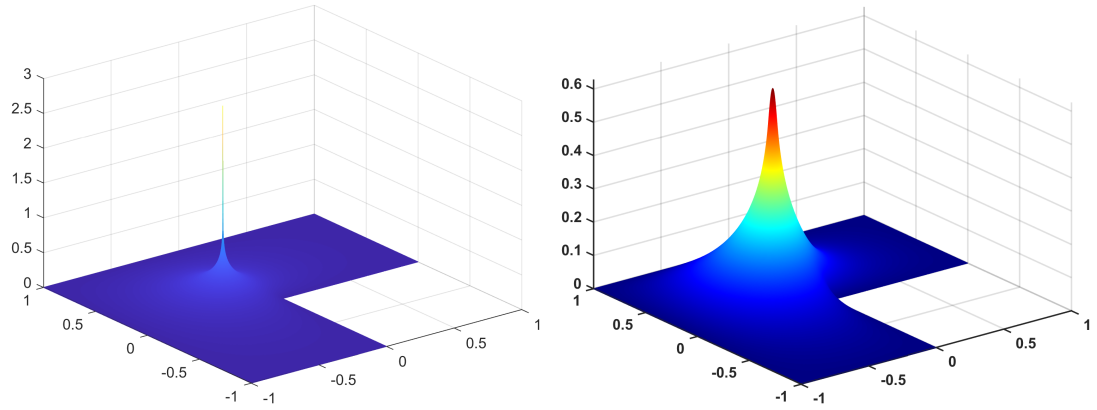

(a) Algorithm 3.1 (b) GOAFEM-MOLL

Figure 7: For the point value $u_2((-0.25,0.25))$, discrete dual solutions of Algorithm 3.1 and GOAFEM-MOLL.

gorithm 3.1 and GOAFEM-MOLL for the point value $u_2((-0.25,0.25))$, where the second subscript of their quantities is A. We see that, for Algorithm 3.1, the error and the error estimator both exhibit the monotonic reduction at the expected rate, but for GOAFEM-MOLL, the errors $|Q_{x_1,\epsilon}(u)-Q_{x_1,\epsilon}(u_{h,1})|$ and $|u(\boldsymbol{x}_1)-u_{h,1}(\boldsymbol{x}_1)|$ are identical and nonmonotonically decreasing.

Fig. 8 also plots the corresponding results of two algorithms whose marking strategies are both replaced by Strategy B (see Remark 3.3) and whose quantities are with the second subscript B. We observe that the point error of Algorithm 3.1 no longer stays monotone-decreasing and the one of GOAFEM-MOLL is still a nonmonotonic sawtooth reduction.

The above results indicate that, in this numerical example, Algorithm 3.1 can preserve

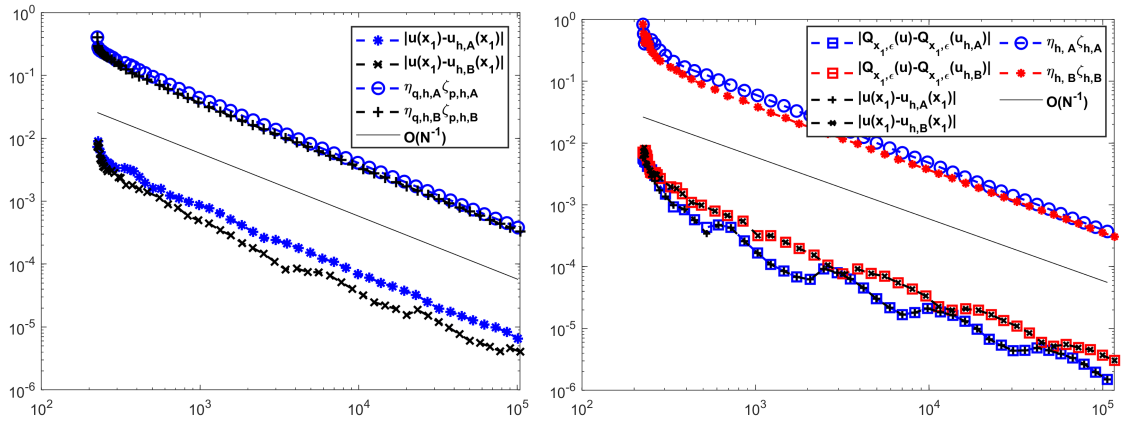

(a) Algorithm 3.1 (b) GOAFEM-MOLL

Figure 8: For point value $u_2((-0.25,0.25))$, errors and error estimator versus the number of mesh vertices for Algorithm 3.1 and GOAFEM-MOLL based on Strategy A and B.

the monotonicity of the error reduction in the pointwise quantity of interest, which is important in adaptivity, but GOAFEM-MOLL cannot.

Example 4.3. In this example, we test Algorithm 3.1 for two points of interest. Select the domain $\Omega=(0,1)\times(0,1)$ and the matrix $a=\begin{pmatrix} x+y & 0 \\ 0 & x+y \end{pmatrix}$ in (2.1a). The corresponding analytical solution is

$$u=100e^{-10000((x-0.25)^2+(y-0.25)^2)}+10e^{-1000((x-0.75)^2+(y-0.75)^2)},$$

which is a double peak with the centers $\boldsymbol{x}_1=(0.25,0.25)$ and $\boldsymbol{x}_2=(0.75,0.75)$, and the associated strengths 10000 and 1000, respectively. We consider the following quantity of interest

$$Q_{\boldsymbol{x}_1,\boldsymbol{x}_2}(u)=\frac{1}{2}(u(\boldsymbol{x}_1)+u(\boldsymbol{x}_2)),$$

which is the mean-value of the solution u at two points $\boldsymbol{x}_1$ and $\boldsymbol{x}_2$. Choose also $p=1.5$ for Algorithm 3.1.

The adaptive mesh and the corresponding discrete dual solution as well as errors and the error estimator of Algorithm 3.1 for the quantity of interest $Q_{\boldsymbol{x}_1,\boldsymbol{x}_2}(u)$ are shown in Fig. 9, from which we observe that the discrete dual solution is also a double peak, and that not only the mean-value error $|Q_{\boldsymbol{x}_1,\boldsymbol{x}_2}(u)-Q_{\boldsymbol{x}_1,\boldsymbol{x}_2}(u_h)|$ as well as its error estimator $\eta_{q,h}\zeta_{p,h}$, but also the pointwise errors $|u(\boldsymbol{x}_1)-u_h(\boldsymbol{x}_1)|$ and $|u(\boldsymbol{x}_2)-u_h(\boldsymbol{x}_2)|$ exhibit monotonic reductions at the expected rate $\mathcal{O}(N^{-1})$. This illustrates that Algorithm 3.1 is valid in the example.

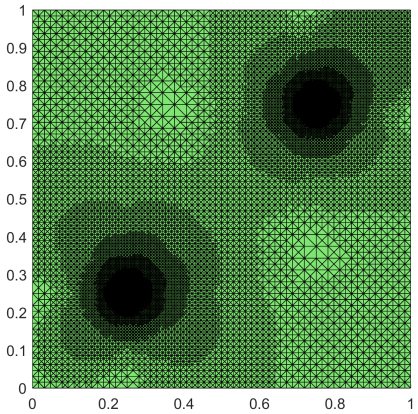

(a) Adaptive mesh

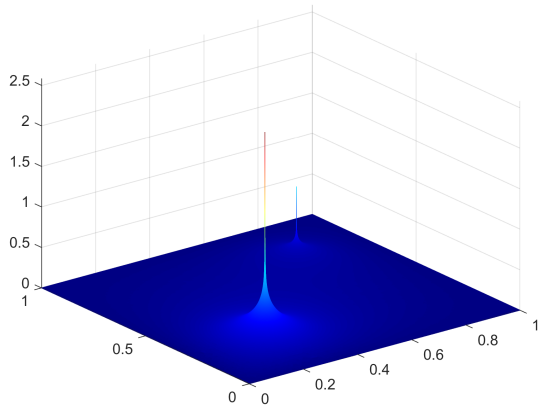

(b) Discrete dual soluion

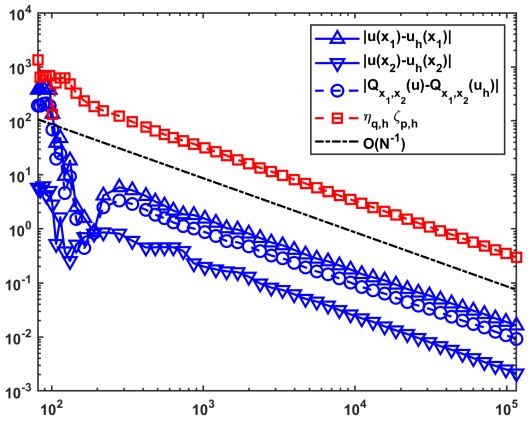

(c) Error and error estimator

Figure 9: Numerical results of Example 4.3.

Acknowledgements

Li's research was partially supported by the Hunan Provincial Innovation Foundation for Postgraduate (No. CX20190462) and the Research and Cultivation Foundation for Young Teachers of South China Normal University (No. 22KJ26); Liu's research was partially supported by National Independent Innovation Demonstration Area-Changsha, Zhuzhou & Xiangtan Project (No. 2018XK2302); Yi's research was partially supported by the National Natural Science Foundation of China (Nos. 12071400 and 11971410) and China's National Key R&D Programs (No. 2020YFA0713500); Zhong's research was partially supported by the National Natural Science Foundation of China (No. 12071160).

References

[1] M. AINSWORTH AND J. T. ODEN, A Posteriori Error Estimation in Finite Element Analysis, Wiley, 2000.

[2] A. ALLENDES, E. OTÁROLA, R. RANKIN, AND A. J. SALGADO, *Adaptive finite element methods for an optimal control problem involving Dirac measures,* Numer. Math., 137(1) (2017), pp. 159–197.

[3] R. ARAYA, E. BEHRENS, AND R. RODRÍGUEZ, *A posteriori error estimates for elliptic problems with Dirac delta source terms,* Numer. Math., 105(2) (2006), pp. 193–216.

[4] W. BANGERTH AND R. RANNACHER, Adaptive Finite Element Methods for Differential Equations, Birkhäuser Verlag, Basel, 2003.

[5] R. BECKER, G. GANTNER, M. INNERBERGER, AND D. PRAETORIUS, *Goal-oriented adaptive finite element methods with optimal computational complexity,* Numer. Math., 153(1) (2023), pp. 111–140.

[6] R. BECKER AND R. RANNACHER, *An optimal control approach to a posteriori error estimation in finite element methods,* Acta Numer., 10 (2001), pp. 1–102.

[7] S. BRENNER AND R. SCOTT, The Mathematical Theory of Finite Element Methods, Springer, 2007.

[8] Y. CHEN, J. S. HESTHAVEN, Y. MADAY, AND J. RODRÍGUEZ, *Certified reduced basis methods and output bounds for the harmonic Maxwell's equations,* SIAM J. Sci. Comput., 32(2) (2010), pp. 970–996.

[9] P. G. CIARLET, The Finite Element Method for Elliptic Problems, Society for Industrial and Applied Mathematics, Philadelphia, 2002.

[10] K. A. CLIFFE, J. COLLIS, AND P. HOUSTON, *Goal-oriented a posteriori error estimation for the travel time functional in porous media flows,* SIAM J. Sci. Comput., 37(2) (2015), pp. B127–B152.

[11] M. DAUGE, *Neumann and mixed problems on curvilinear polyhedra,* Integr. Equ. Oper. Theory, 15(2) (1992), pp. 227–261.

[12] B. ENDTMAYER, U. LANGER, AND T. WICK, *Two-side a posteriori error estimates for the dual-weighted residual method,* SIAM J. Sci. Comput., 42(1) (2020), pp. A371–A394.

[13] L. C. EVANS, Partial Differential Equations Second Edition, American Mathematical Society, 2010.

[14] M. FEISCHL, D. PRAETORIUS, AND K. G. VAN DER ZEE, *An abstract analysis of optimal goal-oriented adaptivity,* SIAM J. Numer. Anal., 54(3) (2016), pp. 1423–1448.

[15] M. B. GILES AND E. SÜLI, *Adjoint methods for PDEs: a posteriori error analysis and postprocessing by duality,* Acta Numer., 11 (2002), pp. 145–236.

[16] R. HARTMANN, *Multitarget error estimation and adaptivity in aerodynamic flow simulations,* SIAM J. Sci. Comput., 31(1) (2008), pp. 708–731.

[17] M. HOLST AND S. POLLOCK, *Convergence of goal-oriented adaptive finite element methods for nonsymmetric problems,* Numer. Methods Partial Differ. Equ., 32(2) (2016), pp. 479–509.

[18] M. HOLST, S. POLLOCK, AND Y. ZHU, *Convergence of goal-oriented adaptive finite element methods for semilinear problems,* Comput. Vis. Sci., 17(1) (2015), pp. 43–63.

[19] P. HOUSTON AND T. P. WIHLER, *Discontinuous Galerkin methods for problems with Dirac delta source,* ESAIM Math. Model. Numer. Anal., 46(6) (2012), pp. 1467–1483.

[20] G. HU, X. MENG, AND N. YI, *Adjoint-based an adaptive finite volume method for steady Euler equations with non-oscillatory k-exact reconstruction,* Comput. Fluids, 139 (2016), pp. 174–183.

[21] P. INGELSTRÖM AND A. BONDESON, *Goal-oriented error estimation and h-adaptivity for Maxwell's equations,* Comput. Methods Appl. Mech. Eng., 192(22-24) (2003), pp. 2597–2616.

[22] T. KÖPPL AND B. WOHLMUTH, *Optimal a priori error estimates for an elliptic problem with Dirac right-hand side,* SIAM J. Numer. Anal., 52(4) (2014), pp. 1753–1769.
[23] S. KOROTOV, P. NEITTAANMÄKI, AND S. REPIN, *A posteriori error estimation of goal-oriented quantities by the superconvergence patch recovery,* J. Numer. Math., 11(1) (2003), pp. 33–59.
[24] F. LARSSON, P. HANSBO, AND K. RUNESSON, *Strategies for computing goal-oriented a posteriori error measures in non-linear elasticity,* Internat. J. Numer. Methods Eng., 55(8) (2002), pp. 879–894.
[25] F. LI AND N. YI, *A posteriori error estimates of goal-oriented adaptive finite element methods for nonlinear reaction-diffusion problems,* J. Comput. Appl. Math., 412 (2022), 114362.
[26] M. S. MOMMER AND R. STEVENSON, *A goal-oriented adaptive finite element method with convergence rates,* SIAM J. Numer. Anal., 47(2) (2009), pp. 861–886.
[27] J. T. ODEN AND S. PRUDHOMME, *Goal-oriented error estimation and adaptivity for the finite element method,* Comput. Math. Appl., 41(5-6), pp. 735–756.
[28] S. PRUDHOMME AND J. T. ODEN, *On goal-oriented error estimation for elliptic problems: application to the control of pointwise errors,* Comput. Methods Appl. Mech. Eng., 176(1-4) (1999), pp. 313–331.
[29] E. RABIZADEH, A. S. BAGHERZADEH, C. ANITESCU, N. ALAJLAN, AND T. RABCZUK, *Pointwise dual weighted residual based goal-oriented ıt a posteriori error estimation and adaptive mesh refinement in 2D/3D thermo-mechanical multifield problems,* Comput. Methods Appl. Mech. Eng., 359 (2020), 112666.
[30] E. STEIN, M. RÜTER, AND S. OHNIMUS, *Error-controlled adaptive goal-oriented modeling and finite element approximations in elasticity,* Comput. Methods Appl. Mech. Eng., 196(37-40) (2007), pp. 3598–3613.
[31] R. VERFÜRTH, A Posteriori Error Estimation Techniques for Finite Element Methods, Oxford University Press, 2013.
[32] F. XU, Q. HUANG, H. YANG, AND H. MA, *Multilevel correction goal-oriented adaptive finite element method for semilinear elliptic equations,* Appl. Numer. Math., 1722 (2022), pp. 24–241.